Characteristics of Lath Martensite: Part II. The Martensite-Austenite Interface

B. P. J. SANDVIK and C. M. WAYMAN

This investigation, using an Fe-20 pct Ni-5 pct Mn (wt pct) alloy, deals with the nature of the lath martensite-austenite interface. For the first time the misfit dislocation structure associated with a martensite interface has been observed experimentally. The interface consists of a single set of parallel dislocations having Burgers vector $a/2[111]_{martensite} = a/2[011]_{austenite}$. Relative to the austenite, the observed dislocation line direction is $[0\bar{5}7]$, and the dislocation line deviates about 10 and 15 deg from the pure screw orientation in the austenite and martensite, respectively. However, the dislocations are in screw orientation on an atomic scale, although the interface step structure causes them to deviate from the exact screw orientation macroscopically. The spacing of the interface dislocations varies from 26 to 63Å. The observed interface dislocation array satisfies the requirements for a glissile interface, which suggests that the dislocations are misfit dislocations which accomplish the lattice invariant shear of the crystallographic theories.

I. INTRODUCTION

IN spite of the great importance of the structure of the martensite-parent interface in martensitic transformations, very little experimental work has been done on such interfaces. Theoretically, two different kinds of dislocations may exist in the martensite-parent interface.[1,2] One kind of dislocation, termed secondary dislocation by Christian,[1] and coherency dislocation by Olson and Cohen,[2] transforms the parent lattice into the product lattice. The second kind of dislocations accommodate the misfit between the parent and product lattices, and in martensitic transformations they also accomplish the lattice invariant shear needed to establish a macroscopically invariant interface[3,4] between the parent and product lattices. These dislocations are termed primary dislocations by Christian and anticoherency dislocations by Olson and Cohen. In this paper we prefer to use the more descriptive terms transformation dislocations and misfit dislocations for the secondary (coherency) and primary (anticoherency) dislocations, respectively. It is also considered[5] that an irrational semicoherent martensitic interface must consist of steps on adjacent close packed planes.

Since the misfit dislocations, contrary to transformation dislocations, have the same properties as lattice dislocations, they can be studied using conventional transmission electron microscopy techniques. This, of course, requires the spacing of the dislocations to be within the resolution of transmission electron microscopy. Although transformation dislocations have been observed for bcc-twins,[6] fcc-twins,[7] and the fcc → hcp martensite transformation,[8] they are not very likely to be resolvable for the fcc → bcc martensite transformation in Fe-alloys, because calculations[9] show that the Burgers vector is small and the dislocations are very closely spaced. Because of this, and the fact that experimental information about misfit dislocations is more important than experimental information about transformation dislocations, as far as calculations of martensite crystallography using the phenomenological theories[3,4] are concerned, we describe only the misfit dislocations below.

An important property of martensite is that the martensite-parent interface must be able to move conservatively. According to the simplest model, a martensitic interface may consist of a single set of parallel misfit dislocations.[5,10] Conservative movement of the interface then requires the Burgers vector of the dislocation to have a component normal to the interface, except when the dislocations are pure screws. When such an interface glides, the dislocations accomplish the lattice invariant shear of the phenomenological theories.

More complex interface dislocation arrays also may comprise a semicoherent glissile interface.[5,10] One possibility is that all dislocations are parallel, and have the same glide plane, but different Burgers vectors. Another possibility is that all dislocations have the same Burgers vector, but glide in different planes. The resultant shear produced by such dislocation arrays then corresponds to the lattice invariant shear. The latter approach, *i.e.*, dislocations having the same Burgers vector, but different glide planes, has been criticized,[10] because such a case would require two or more dislocation line directions to exist in the interface. From the phenomenological theories[3,4] it follows that the glide planes in martensite and austenite meet edge to edge in the planar interface along an invariant line, which must be the interface dislocation line. Because there is only one invariant line,[3,4] it is difficult to understand how two or more dislocations in different directions could glide.

A fault free martensite lattice can be produced by the movement of the interface only if the interface dislocations have Burgers vectors which are corresponding lattice vectors in the martensite and parent phases.[5,10]

Although misfit dislocations have never been observed experimentally for martensitic interfaces, they have been observed for many other phase boundaries, *e.g.*, in the interface between α-brass and β-brass,[11] in the interfacial structure of bcc Cr-rich precipitates in an fcc Cu-0.3 pct Cr alloy,[12] and in the interface between epitaxial islands of Cu evaporated on thin films of Ni.[13] From the point of view of the present investigation, there is especially one work which deserves mentioning, namely, the work of Cassidy *et al*[14] on

B. P. J. SANDVIK and C. M. WAYMAN, respectively, are Research Associate and Professor in the Department of Metallurgy and Mining Engineering, University of Illinois at Urbana-Champaign, Urbana, IL 61801.

Manuscript submitted April 30, 1982.

the formation of hydrides in vanadium. The crystallography of these hydrides is consistent with the phenomenological theories of martensite formation, suggesting that the transformation takes place by shear, but since the transformation involves the diffusion of hydrogen, it must be considered bainitic rather than martensitic. The spacing and the Burgers vector of a single set of interface dislocations were consistent with the phenomenological theories.[14] Another interesting work is that of Rigsbee and Aaronson[15] on the structure of the interface between ferrite sideplates and austenite in an Fe-2Si-0.6C alloy. These investigators found a single set of interface dislocations having a Burgers vector in the atomic interface $(111)_{fcc} \parallel (011)_{bcc}$, and one set of steps in the interface. It was concluded that the sideplates may not form by a shear transformation, since the Burgers vector of the dislocations lies in the atomic interface.

In the present investigation the main purpose is to obtain information concerning the misfit dislocation structure of the interface between lath martensite and austenite. Such information would not only help to gain a better understanding of the general nature of martensite interfaces, but also provide necessary input data concerning the lattice invariant shear for the application of the phenomenological theories on the formation of lath martensite. The present paper deals with experimental observations on the interface structure, while the theoretically calculated interface structure is obtained in connection with the application of the phenomenological theory as described in a later paper.

II. EXPERIMENTAL

The experimental equipment used in transmission electron microscopy has been described in the previous paper.[16] Both kinds of specimen preparation techniques described in Reference 16 were used in the present investigation.

Because of the commonly occurring close spacing of interface dislocations, the resolution of conventional bright-field transmission electron microscopy is usually too low for the investigation of interface dislocation structures. Significantly higher resolution can be achieved by the application of the weak-beam dark-field method developed by Cockayne.[17] A detailed description of the application of this technique on interface structures has been given by Rigsbee and Aaronson.[15] These investigators estimated the optimum resolution to be about 8Å when a {110} ferrite reflection and 100 kV accelerating voltage are used. Due to the increase in extinction distance, the resolution diminished when higher order reflections were used. The weak-beam dark-field method allows the analysis of Burgers vectors of dislocations to be carried out using the conventional $\bar{g} \cdot \bar{b} = 0$ invisibility criterion.[17]

Mainly two difficulties arise when the weak-beam method is used, both of which are a result of the low intensity of weak-beam images. First, correction of objective astigmatism is difficult, since the interface dislocations are frequently difficult to detect on the screen of the microscope. The astigmatism correction then has to be carried out on coarser features, like dislocations in the martensite or in the austenite. Second, the low intensity of the image usually requires a long exposure time, and image drifting may diminish the quality of the photograph. This difficulty was partly overcome by preparing a developing solution of Kodak HRP developer in the ratio 1:2 instead of the conventional ratio 1:4. When this solution was used an exposure time of 4 to 8 seconds was generally adequate. Although this procedure causes a slight increase in the grain size of the film, the benefit as compared to the use of long exposure times is obvious.

III. RESULTS

A. *General Observations*

Figure 1 shows a weak-beam dark-field electron micrograph taken of a martensite lath in a matrix of austenite using the reflection $(\bar{1}10)_b$.* It is seen that the same single set of parallel dislocations exists in the interface on both sides of the lath. Local changes in the orientation of the interface cause the direction of the dislocation line to vary slightly from region to region, as seen at the side of the interface marked A. For more than 30 laths examined, only one set of parallel dislocations was found in the interface, except for a few laths as those discussed in association with Figures 4 and 5. As will be shown later, all dislocations in the single set of interface dislocations have the same Burgers vector.

The image contrast of the interface dislocations is very sensitive to the diffraction condition. In contrast to the exceptionally thin lath in Figure 1, laths of normal thickness

*In this paper all crystallographic information is given in terms of the following variant of the austenite-martensite orientation relationship: $(111)_f \| (011)_b$ and $[\bar{1}01]_f$ 3.9 deg from $[\bar{1}\bar{1}1]_b$.

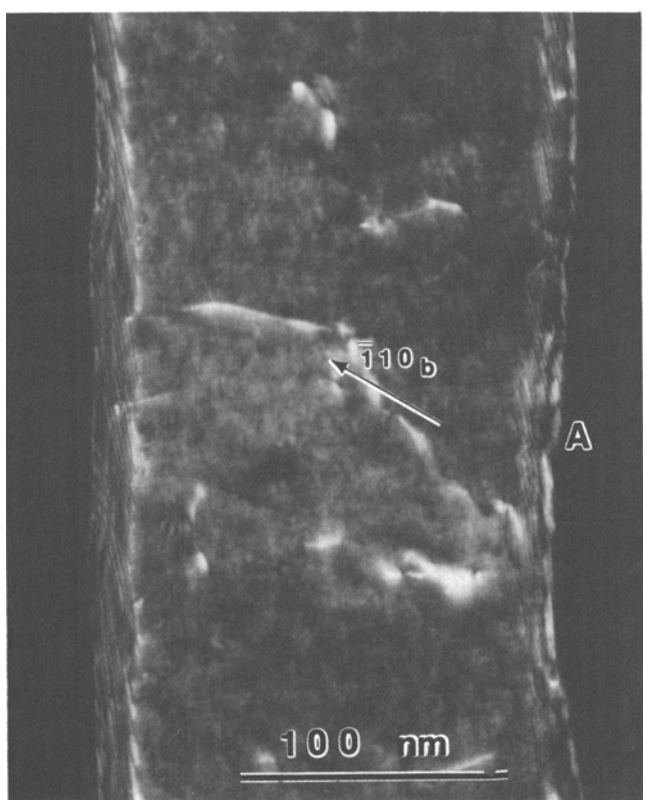

Fig. 1 — Weak-beam image obtained using the $(\bar{1}10)_b$ reflection showing a single set of parallel interface dislocations on both sides of a martensite lath. Local changes in the dislocation line direction can be seen on the side of the interface marked A.

(~0.3 μm) usually had to be tilted for separate examination of the two sides of the lath.

Because an interface dislocation, like a line dislocation, cannot end within a crystal, the dislocations probably form loops around the laths. Figure 2 shows the interface dislocation structure very close to a lath edge. Also, this micrograph shows only one set of interface dislocations. The dislocations at the arrow A are internal martensite dislocations, the projected images of which partly overlap with the projected image of the interface. There are also some local irregularities in the interface orientation, as indicated by the arrows B. This figure shows that the martensite lath edges may be rounded, *i.e.*, the interface plane is successively rotated toward the lath edge. Since the martensite/austenite interface also broadens toward the lath edge, the interface plane is both curved and twisted.

Although it would be valuable to obtain detailed information concerning the interface structure at lath edges, such an investigation could not be carried out because it was impossible to obtain good contrast from the lath edges. This is obviously due to considerable elastic strain at the lath edges. Nevertheless, since the dislocation structure close to lath edges has the same configuration as that at the broad faces of the laths, it is suggested that the dislocations form loops around the laths.

Figure 3 shows a weak-beam image of a lath edge. The morphology appears to be rather complex, and the edge of the lath is segmented. In spite of the difficulty to obtain a good image of lath edges, a single set of dislocations can be observed, and the dislocation lines appear to be continuous with the dislocation lines farther away from the lath edge, again suggesting that the dislocations form loops around the laths.

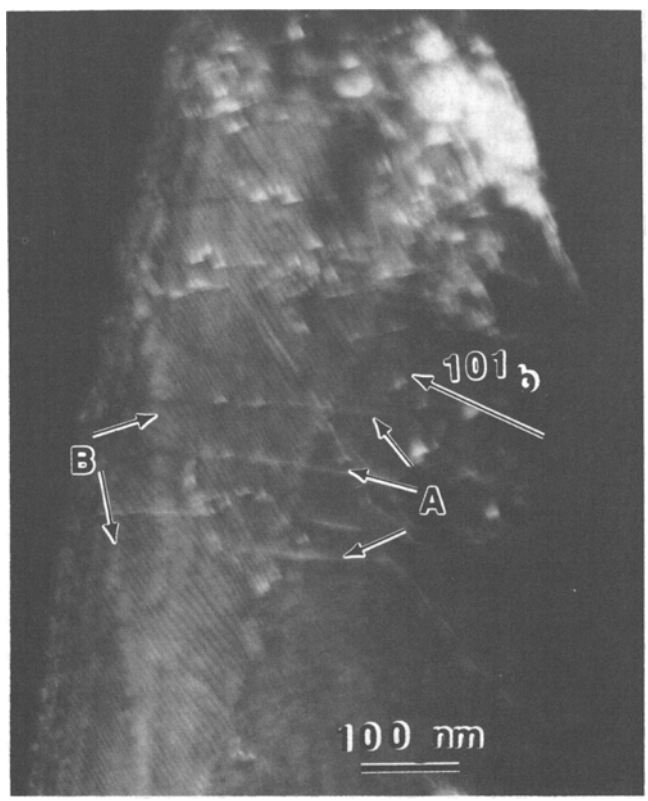

Fig. 2 — Weak-beam image obtained using the $(101)_b$ reflection showing a single set of parallel interface dislocations at a lath edge. The arrows A indicate internal martensite dislocations, while the arrows B indicate irregularities in the interface.

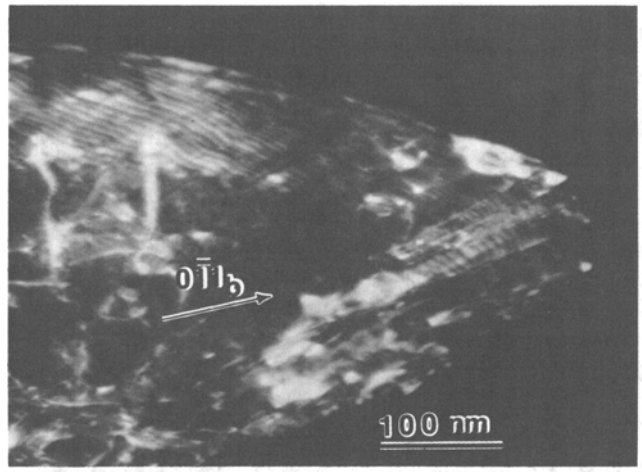

Fig. 3 — Weak-beam image obtained using the $(0\bar{1}1)_b$ reflection showing a segmented lath edge and a single set of parallel interface dislocations.

An even more complex structure close to a lath edge is shown in Figure 4, in which the interface dislocation lines appear light. The spacing of the dislocations is rather irregular at some regions, and the direction of the dislocation lines varies, indicating that the interface is not planar. The line features having the direction $[\bar{1}\,\bar{1}1]_b$ are probably internal dislocations which have moved to the interface. An interesting notion is that the projected width of the interface on the lower side of the lath is much larger than the projected width of the interface on the upper side of the lath. This shows that the interface planes on the two sides of the lath are separated by a wide angle. Such situations were not observed at large distances from lath edges.

Figure 5 shows the interface of a broad side of a lath. In addition to the very regular interface dislocation array, there is also a set of irregularly spaced dislocations having the direction $[\bar{1}\,\bar{1}1]_b$. These dislocations appear to be internal dislocations which have moved to the interface.

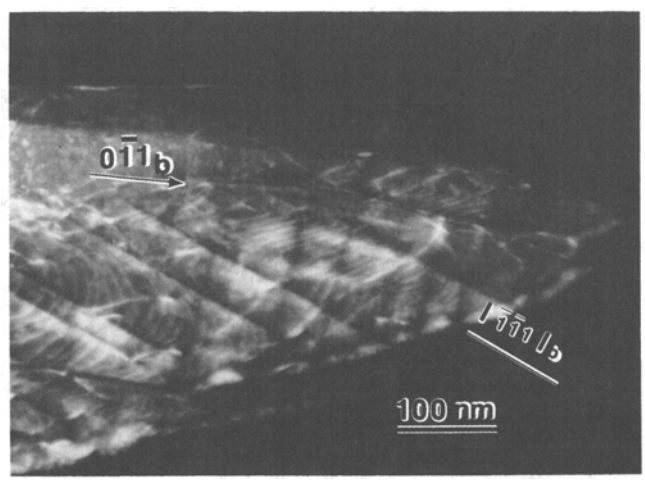

Fig. 4 — Weak-beam image obtained using the $(0\bar{1}1)_b$ reflection showing complex interface dislocation structure and line features having the direction $[\bar{1}\bar{1}1]_b$.

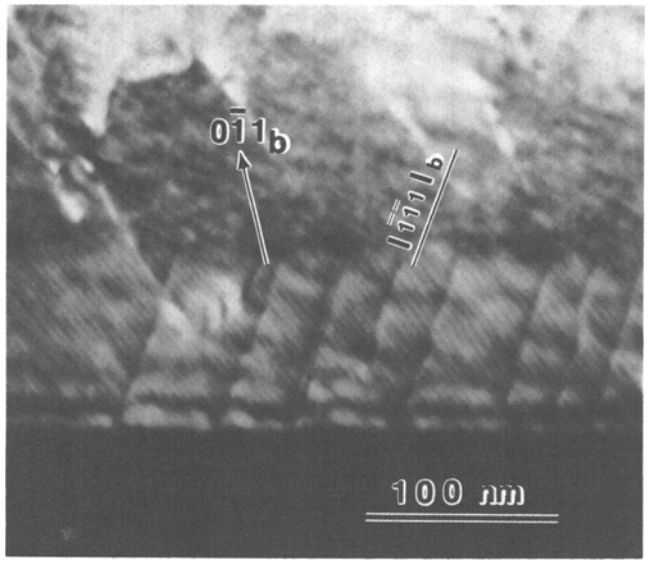

Fig. 5—Weak-beam image obtained using the $(0\bar{1}1)_b$ reflection showing 1 set of regularly spaced interface dislocations and 1 set of irregularly spaced interface dislocations.

When interfaces are investigated, great care has to be taken in order to distinguish interface dislocations from moiré fringe patterns, which may appear very similar to the image contrast of interface dislocations. The dislocations investigated in this work are a reproducible feature of the laths, and the same array of interface dislocations is always found in different laths. Thus, laths could be studied in various orientations, and the dislocations were imaged using many different reflections without any change in configuration. Figure 1 showed that the direction of the features may vary with variations in interface orientation. This is not typical of moiré fringe patterns. Another feature typical of dislocations is that a dislocation may end into another dislocation. The arrows in Figure 6 indicate interface dislocations which terminate into internal martensite dislocations at the left side of the arrows. Accordingly, it appears to be quite clear that the observed structure is a dislocation structure.

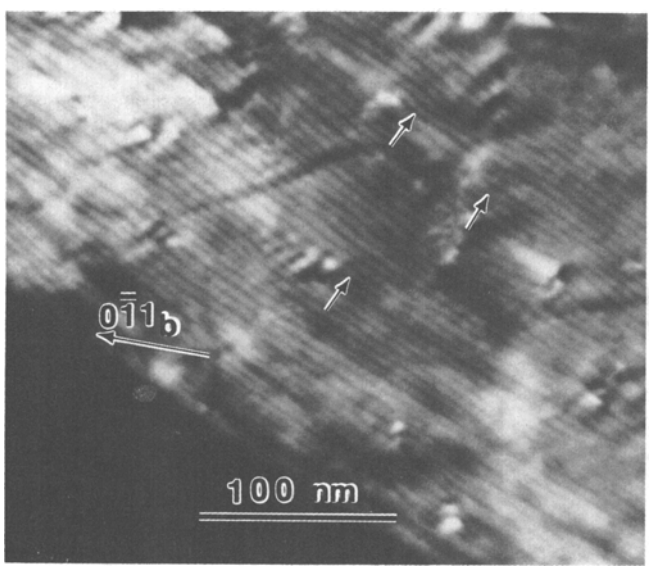

Fig. 6—Weak-beam image obtained using the $(0\bar{1}1)_b$ reflection. The arrows indicate interface dislocations which terminate into internal martensite dislocations.

B. *Determination of Burgers Vectors*

In the determination of the Burgers vector, the correct variant of the foil orientation could be determined from the austenite-martensite orientation relationship[16] and the direction of the dislocation line described in the following section.

Figure 7 shows the interface of a lath in a specimen having an orientation close to $[\bar{1}11]_b$ and $[011]_f$. The micrographs in Figures 7(a) and 7(b) are taken using the reflections $(0\bar{1}1)_b$ and $(1\bar{1}1)_f$, respectively. Dislocations are visible in both martensite and austenite, indicating that the dislocations have a Burgers vector which is defined in both phases. Figure 8 shows another lath in the same orientation.

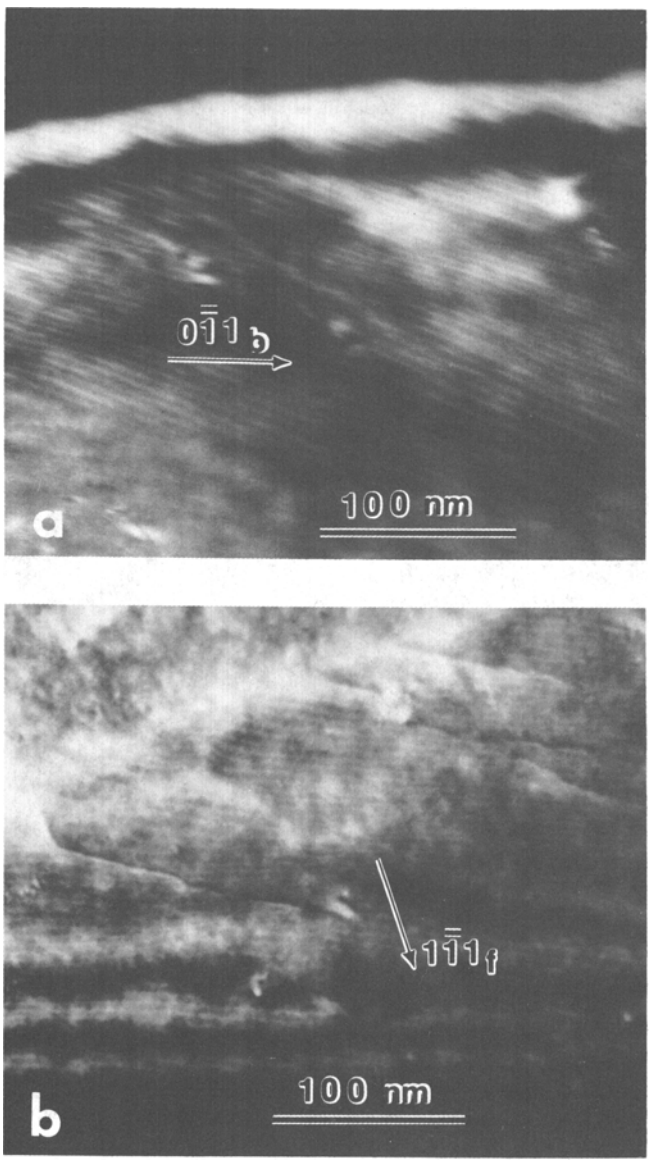

Fig. 7—Weak-beam images of dislocations showing contrast in both martensite and austenite: (*a*) is taken using the $(0\bar{1}1)_b$ reflection, and (*b*) is taken using the $(1\bar{1}1)_f$ reflection. The foil orientation is close to $[\bar{1}11]_b$ and $[011]_f$.

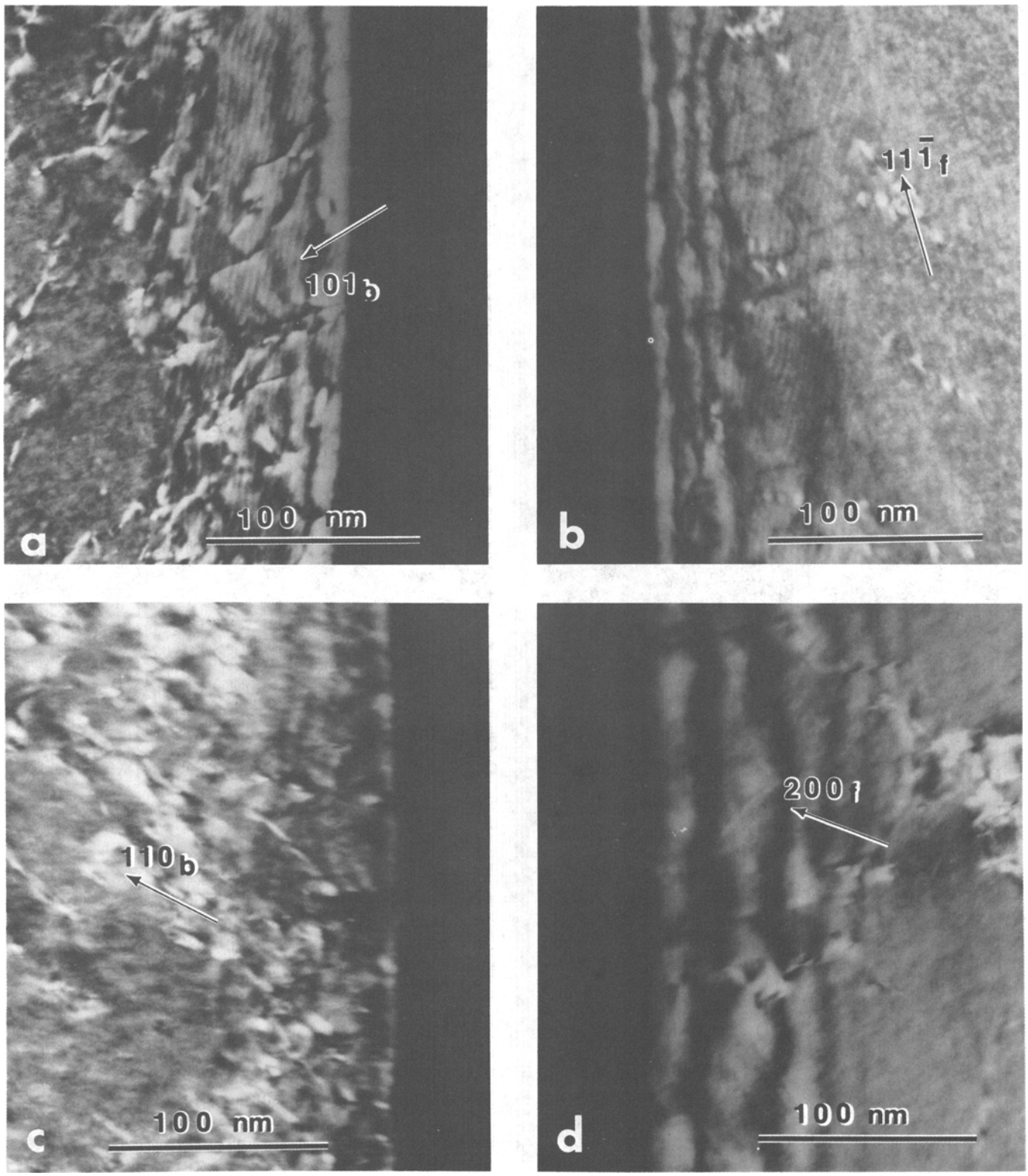

Fig. 8 — Weak-beam images of interface dislocations obtained using the following reflections: (*a*) $(101)_b$, (*b*) $(11\bar{1})_f$, (*c*) $(110)_b$, and (*d*) $(200)_f$. The foil orientation is close to $[\bar{1}11]_b$ and $[011]_f$.

Figures 8(a) and 8(b) are taken by the reflections $(101)_b$ and $(11\bar{1})_f$, respectively. Again the dislocations show contrast in both phases. In Figures 8(c) and 8(d), which are taken using the reflections $(110)_b$ and $(200)_f$, however, the dislocations go out of contrast in both martensite and austenite.

The micrographs shown in Figure 9 are taken using the electron beam orientations $[\bar{1}11]_b$ and $[\bar{1}31]_b$, and the reflections used are indicated in the micrographs. Interface dislocations are visible for the reflections $(0\bar{1}1)_b$ and $(\bar{1}\,\bar{1}2)_b$, but invisible for the reflections $(110)_b$ and $(21\bar{1})_b$. This figure

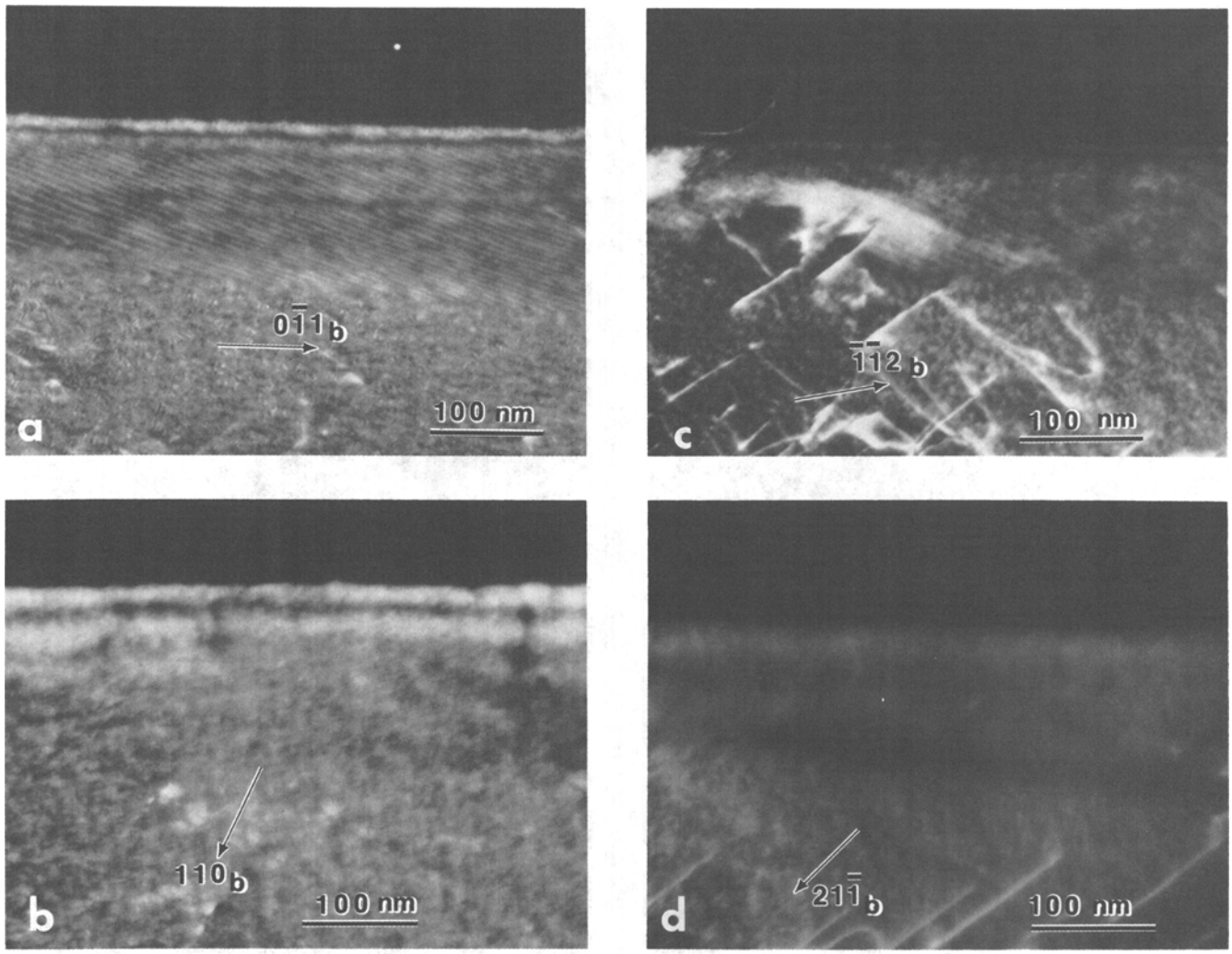

Fig. 9—Weak-beam images of interface dislocations obtained using the following reflections: (*a*) $(0\bar{1}1)_b$, (*b*) $(110)_b$, (*c*) $(\bar{1}\bar{1}2)_b$, and (*d*) $(21\bar{1})_b$. The foil orientation is approximately $[\bar{1}11]_b$ in (a) and (b) and $[\bar{1}31]_b$ in (c) and (d).

demonstrates that the resolution is high enough to resolve dislocations using $\{211\}_b$ type reflections. For the lath in Figure 9 the interface dislocations were also visible when imaged by the reflections $(101)_b$, $(020)_b$, and $(\bar{1}2\bar{1})_b$.

Figure 10 shows a lath photographed using the electron beam orientation $[10\bar{1}]_b$. Interface dislocations are visible for the operating reflection $(\bar{1}2\bar{1})_b$, but invisible for the reflection $(121)_b$. The dislocations were also visible for the reflections $(01\bar{1})_b$ and $(101)_b$. Finally, Figure 11 shows a lath in a foil with the orientation $[111]_b$. The dislocations are visible in Figure 11(a), taken using the reflection $(01\bar{1})_b$ and invisible in Figure 11(b), taken using the reflection $(\bar{1}01)_b$. The dislocations were also visible for the reflection $(\bar{1}10)_b$.

In summary, the dislocations are visible when imaged using the reflections $(01\bar{1})_b$, $(101)_b$, $(\bar{1}10)_b$, $(020)_b$, $(\bar{1}\bar{1}2)_b$, and $(\bar{1}2\bar{1})_b$, and invisible when imaged using the reflections $(\bar{1}01)_b$, $(110)_b$, $(121)_b$, and $(21\bar{1})_b$. This shows quite uniquely that the Burgers vector of the dislocations must be $a_b/2\ [1\bar{1}1]_b$. There is only one set of resolvable interface dislocations, and all dislocations have the same Burgers vector. The reflection $(011)_b \| (111)_f$, although contained in the $[1\bar{1}1]$ zone, could not be used for making the dislocations go out of contrast, because the laths are close to being edge-on when this reflection is present in the diffraction pattern.

The Burgers vector analysis was not as complete in the austenite as in the martensite. Only the reflections $(1\bar{1}1)_f$, $(11\bar{1})_f$, and $(200)_f$ were applied (Figures 7 and 8). The dislocations are visible for the reflections $(1\bar{1}1)_f$ and $(11\bar{1})_f$, but invisible for the reflection $(200)_f$. This was confirmed for several laths. Because the Burgers vector in the martensite, $a_b/2\ [1\bar{1}1]_b$, is a conventional bcc lattice dislocation, also the Burgers vector in the austenite may be expected to be a conventional lattice dislocation, *i.e.*, of the type $a_f/2\ \langle 110\rangle$. Since the dislocations are invisible for the reflection $(200)_f$, the Burgers vector must be contained in the $[100]_f$ zone. This zone contains only two close packed directions: $[011]_f$ and $[0\bar{1}1]_f$. Because the Burgers vector $a_f/2\ [011]$ should be invisible for the reflections $(1\bar{1}1)_f$ and $(11\bar{1})_f$, the austenite Burgers vector must be $a_f/2\ [0\bar{1}1]$. Thus, it is concluded that the Burgers vector of the interface dislocations is $a_b/2\ [1\bar{1}1] = a_f/2\ [0\bar{1}1]_f$.

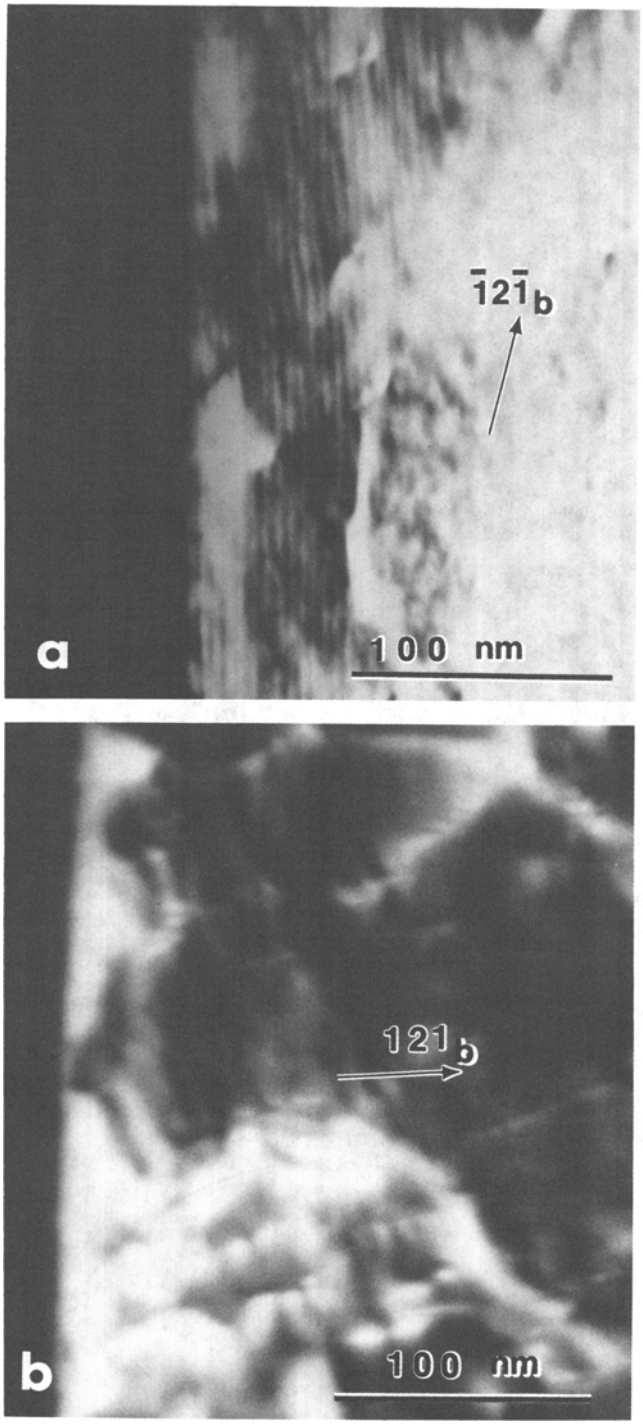

Fig. 10 — Weak-beam images of interface dislocations obtained using the following reflections: (*a*) $(\bar{1}2\bar{1})_b$ and (*b*) $(121)_b$. The foil orientation is close to $[10\bar{1}]_b$.

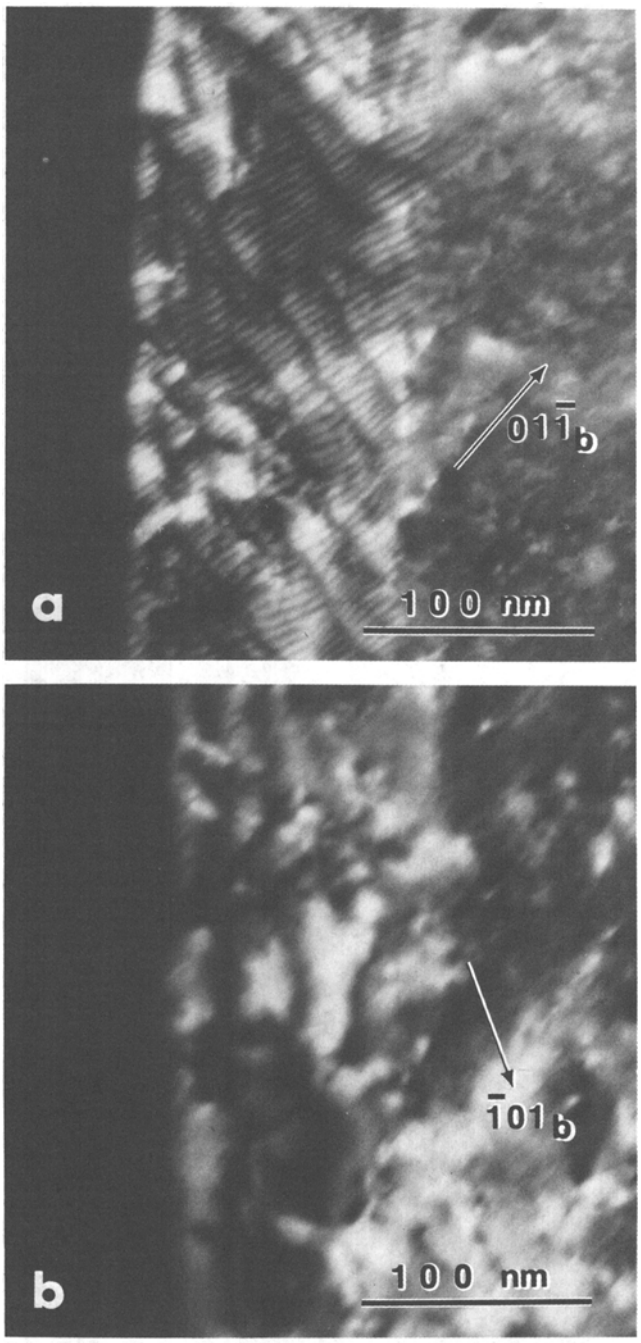

Fig. 11 — Weak-beam images of interface dislocations obtained using the following reflections: (*a*) $(01\bar{1})_b$ and (*b*) $(\bar{1}01)_b$. The foil orientation is close to $[111]_b$.

C. *Determination of the Direction of the Dislocation Line*

The dislocation line direction was determined using conventional trace analysis[18] and at least four widely spaced orientations. Only straight interfaces exhibiting straight dislocations were used for this purpose. Most of the specimens used had the specimen surface orientation close to $[\bar{1}11]_b$ or $[011]_f$, but also orientations such as $[111]_b$ close to $[101]_f$ and $[001]_b$ close to $[001]_f$ were used. The orientations $[111]_b$ and $[\bar{1}11]_b$ can be distinguished on the basis of the approximate dislocation line direction, but also on the basis of the fact that the dislocations are invisible for the reflection $(110)_b$ close to $(200)_f$, but visible for the reflection $(\bar{1}10)_b$ close to $(020)_f$.

The trace analysis was performed by imaging the dislocations using a $\{110\}_b$ reflection, which lies as close as possible to the approximate dislocation line direction. When a reflection which lies close to the dislocation line direction is used, the projected line direction changes more strongly when the specimen is tilted, than when a reflection lying almost 90 deg from the dislocation line direction is used. Thus, the accuracy of the method is higher when a reflection

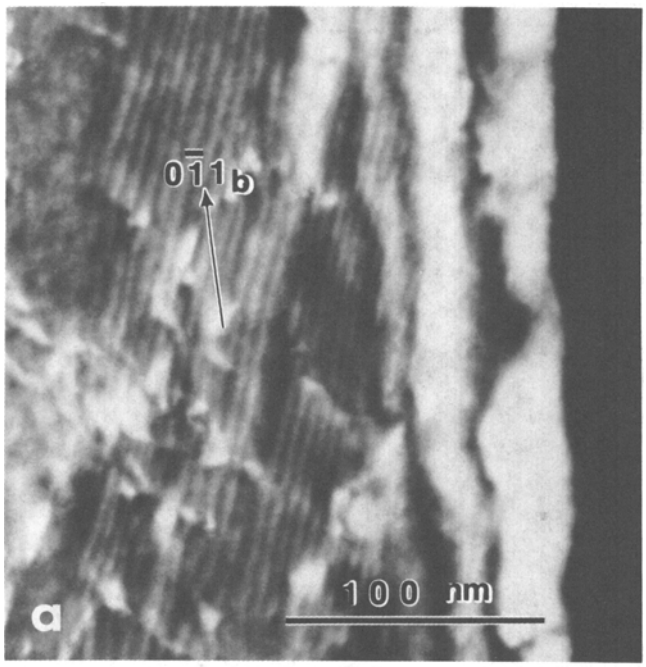

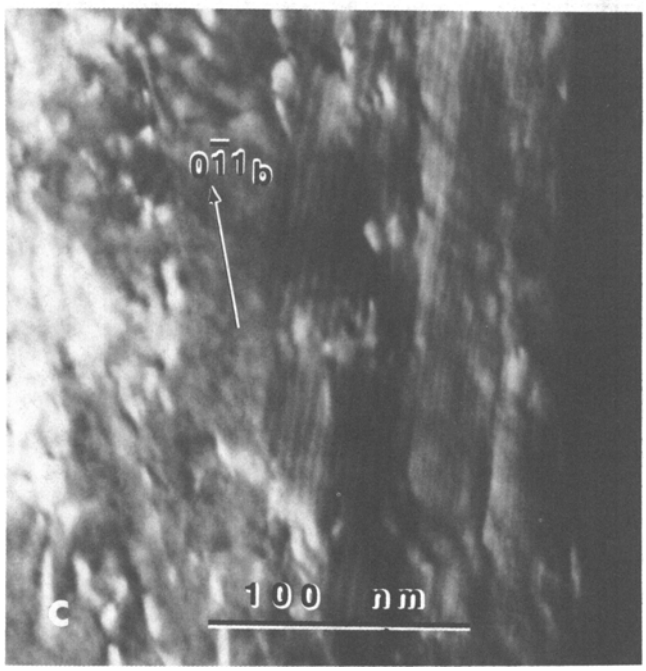

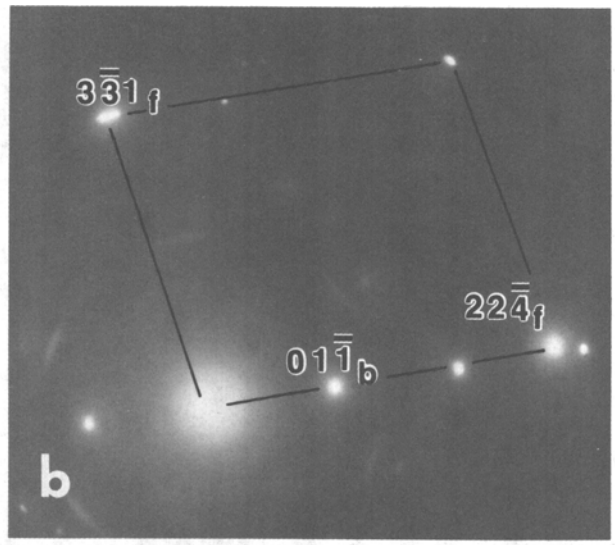

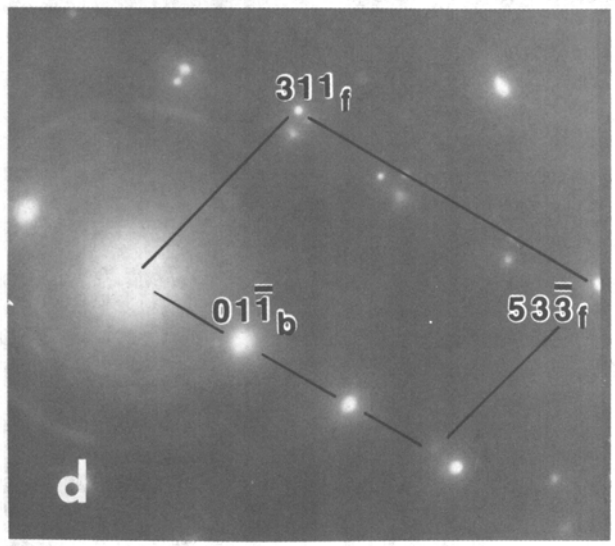

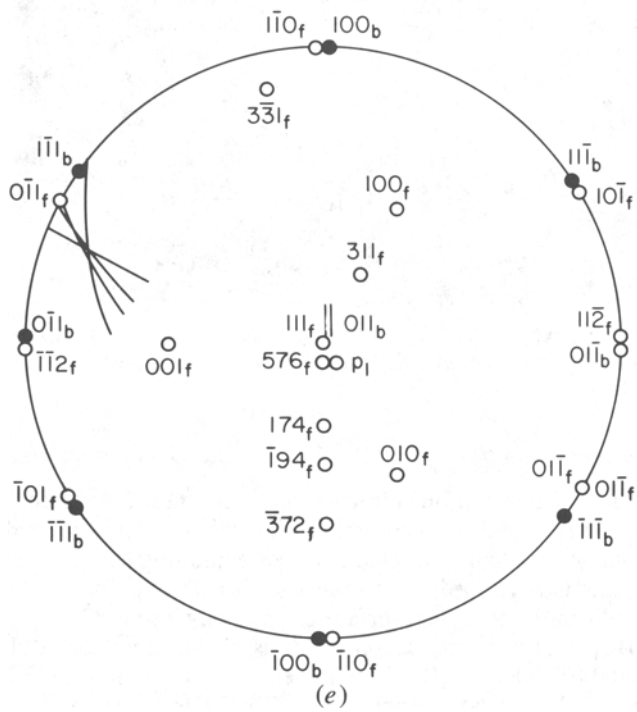

Fig. 12—Determination of interface dislocation line direction: (*a*) weak-beam image of interface obtained using the $(0\bar{1}1)_b$ reflection, (*b*) the corresponding SAD-pattern, (*c*) weak-beam image of interface obtained using the $(0\bar{1}1)_b$ reflection after tilting by an angle of 56 deg from the orientation in (a) and (b), (*d*) the corresponding SAD-pattern, and (*e*) trace analysis of the dislocation line direction using the orientations $[576]_f$, $[174]_f$, $[\bar{1}94]_f$, and $[\bar{3}72]_f$.

close to the dislocation line direction is used. The specimen orientation was determined from high-order austenite zones in the same way as in connection with the habit plane analysis described in Reference 16. The results of one analysis are shown in Figure 12. In this case the dislocations were imaged using the reflection $(0\bar{1}1)_b$, and the orientations used were $[576]_f$, $[174]_f$, $[\bar{1}94]_f$, and $[\bar{3}72]_f$, *i.e.*, the total tilt angle was 56 deg. Usually total tilt angles larger than

45 deg were used. In Figures 12(a) to (d) only the two extreme orientations, $[575]_f$ and $[\bar{3}72]_f$, are shown. Because of the large tilt angles required in order to achieve a reasonable accuracy, the limited resolution allowed only local regions of a lath, exhibiting rather large dislocation spacings, to be examined.

In order to make the results more complete, another method was also applied. The projection of the dislocation line was determined in an orientation close to the untilted condition, after which the habit plane of the lath was determined by tilting the lath edge-on as described in Reference 16. Thus, the true direction of the dislocation line was obtained from the intersection between the habit plane and the projection of the dislocation line.

The results of all analyses are summarized in Figure 13. The experimentally determined habit plane,[16] $(575)_f$, is also plotted in Figure 13. The average dislocation line direction is close to $[0\bar{5}7]_f$. It then follows that the dislocation line direction deviates by about 10 deg from the screw orientation in the austenite, and by about 15 deg from the screw orientation in the martensite.

Figure 14 demonstrates that both the Burgers vector and the line direction of the dislocations are uniquely defined in terms of the accurate variant of the austenite-martensite orientation relationship. The foil orientation in Figure 14(a) is close to $[\bar{1}11]_b$ (Figure 14(c)), and the operating reflection is $(0\bar{1}1)_b$. When imaged using the reflection $(110)_b$, the dislocations are invisible (Figure 14(b)), indicating that the Burgers vector is $a_b/2[1\bar{1}1]$. The accurate variant of the austenite-martensite orientation relationship is obtained when the lath is tilted to the orientation $[111]_f \| [011]_b$ (Figure 14(d)). The stereographic representation of Figures 14(a) to (d) is shown in Figure 14(e). Analyses such as that in Figure 14 were reproduced several times.

D. *Determination of the True Spacing of the Dislocation*

As shown by Howell *et al,*[19] the determination of the true spacing of interface dislocations in tilted specimens is a rather complex procedure, which requires accurate knowledge about parameters like the tilt component about the normal to the foil/habit plane intersection. In order to avoid experimental error arising from inaccuracies in these parameters, the true spacing of the dislocations was studied using only untilted specimens.

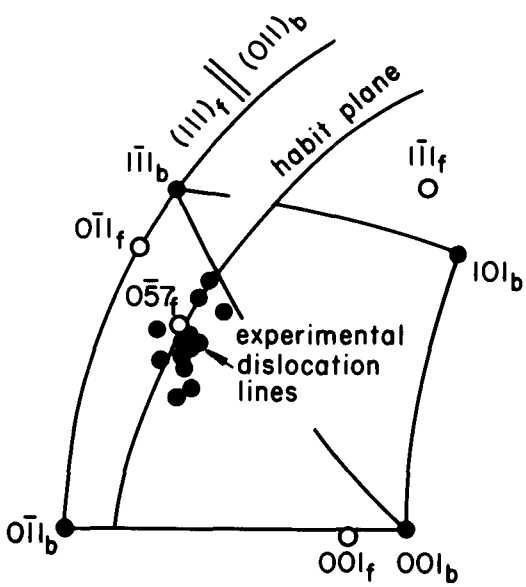

Fig. 13—Experimentally measured interface dislocation line directions for 13 different laths. The average dislocation line direction is close to $[0\bar{5}7]_f$.

In a case like that shown in Figure 8(a), where the foil is essentially untilted, the true spacing (S_t) can be obtained using the formula $S_t = S_p\ (\sin^2\omega/\cos^2\theta + \cos^2\omega)^{1/2}$,[19] where S_p is the projected dislocation spacing, θ is the angle between the plane of the foil surface and the habit plane, and ω is the angle between the projected dislocation line and the normal to the projected foil/habit plane intersection. For the dislocations in Figure 8(a), which have a projected spacing of about 35 Å, a true spacing of 39 Å is obtained since the angle between the electron beam direction $[\bar{1}11]$ and the approximate habit plane normal $[575]_f$ is 27 deg. Seven other cases of the same kind yielded true dislocation spacings ranging between 26 and 63 Å.

In Figure 15 dislocations are seen to lie almost perpendicular to the foil/habit plane intersection in an untilted foil. In this case the true spacing is equivalent to the projected spacing. The average spacing of the dislocations in Figure 15, which was the only observation of this kind, is about 37 Å.

Finally, an estimate of the true dislocation spacing can be directly obtained by tilting the specimen to a position where the electron beam direction is close to the habit plane normal. Such a case is shown in Figure 12(a), where the electron beam orientation $[576]_f$ is only about 5 deg from the average habit plane normal $[575]_f$. The dislocation spacing in Figure 12(a) is about 58 Å. For five other cases of this kind spacings ranging from 41 to 57 Å were measured. The average result obtained by this method, however, is likely to be an overestimate. Tilting the specimen to an orientation close to the habit plane normal requires a rather high angle of tilting for the foil surface orientations used, and only in local regions of the laths, where the dislocation spacing is comparatively large, can the dislocations be resolved. In any event, true dislocation spacings ranging from 26 to 63 Å were observed. The average value obtained from all measurements is 45 Å.

IV. DISCUSSION

For the first time the misfit dislocation structure of a martensitic interface has been observed experimentally. The lath-martensite/austenite interface consists of a single set of parallel dislocations, which all have the same Burgers vector. This situation corresponds to the most simple theoretical model of a semicoherent glissile interface as described by Christian.[5,10] Because no twins or stacking faults were found in the lath martensite,[16] conservative movement of the interface also requires the Burgers vector of the dislocations to be corresponding lattice vectors in martensite and austenite.[5,10] The Burgers vector of the interface dislocations $a_b/2\ [1\bar{1}1] = a_f/2\ [011]$, is in a close-packed direction in both martensite and austenite, and the directions $[\bar{1}11]_b$ and $[0\bar{1}1]_f$ are only about 6.6 deg apart according to the experimentally determined orientation relationship.[16] This suggests that the Burgers vectors of the dislocations

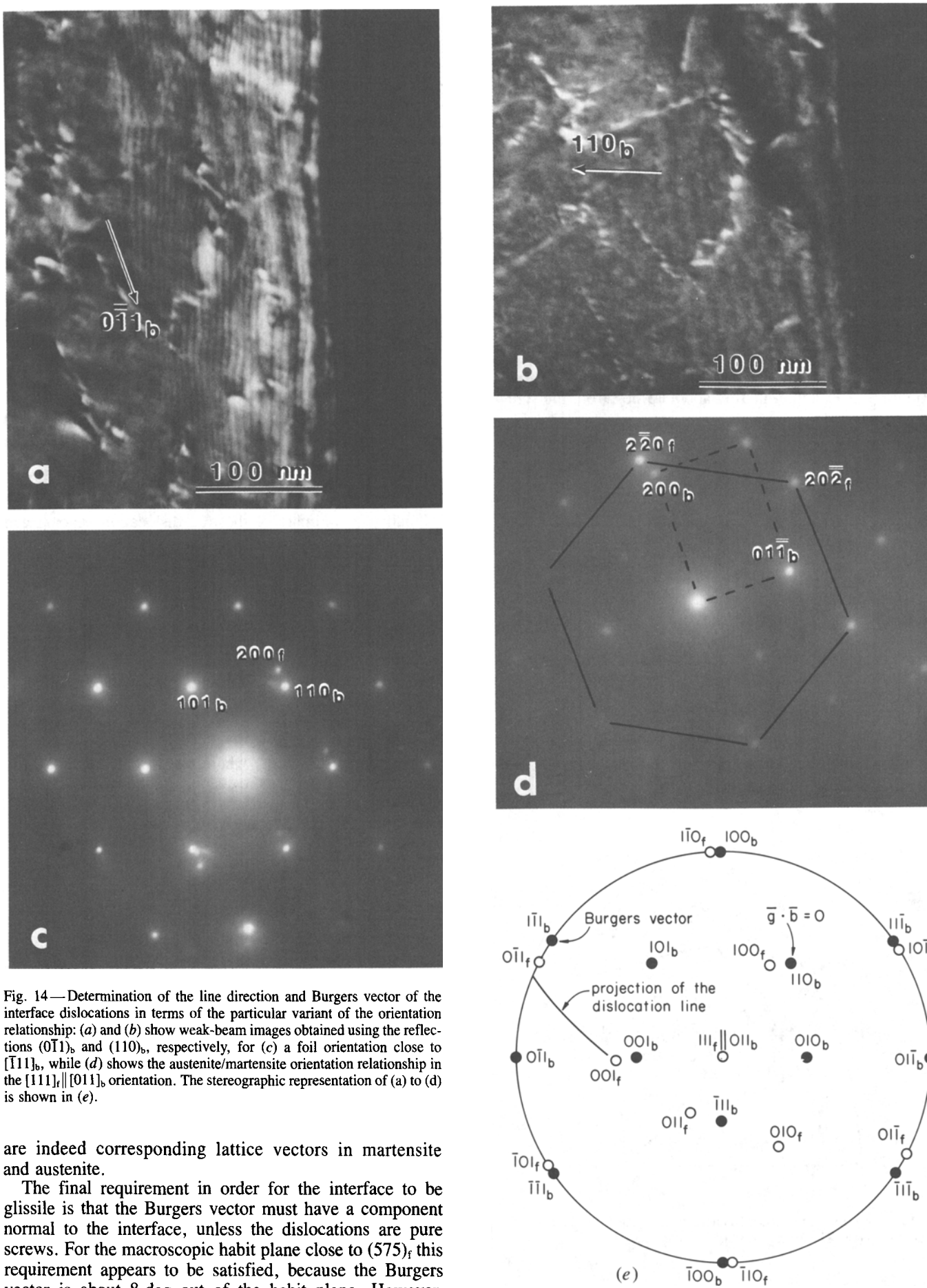

Fig. 14 — Determination of the line direction and Burgers vector of the interface dislocations in terms of the particular variant of the orientation relationship: (*a*) and (*b*) show weak-beam images obtained using the reflections $(0\bar{1}1)_b$ and $(110)_b$, respectively, for (*c*) a foil orientation close to $[\bar{1}11]_b$, while (*d*) shows the austenite/martensite orientation relationship in the $[111]_f \| [011]_b$ orientation. The stereographic representation of (a) to (d) is shown in (*e*).

are indeed corresponding lattice vectors in martensite and austenite.

The final requirement in order for the interface to be glissile is that the Burgers vector must have a component normal to the interface, unless the dislocations are pure screws. For the macroscopic habit plane close to $(575)_f$ this requirement appears to be satisfied, because the Burgers vector is about 8 deg out of the habit plane. However,

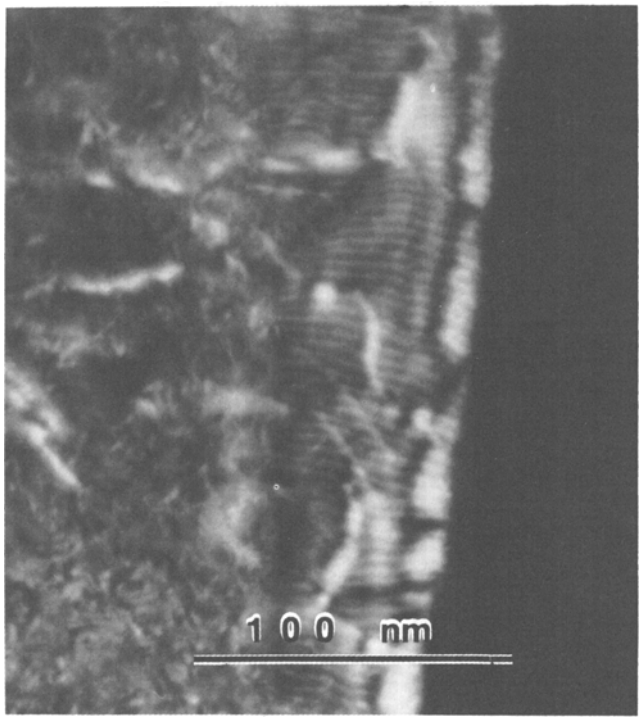

Fig. 15—Weak-beam image of interface dislocations lying perpendicular to the foil/habit plane intersection and having an average spacing of about 37Å.

as pointed out by Christian and Knowles,[5] an irrational semicoherent interface must consist of steps on adjacent close packed planes. Because the habit plane is close to $(111)_f$, the broad surfaces of these steps must be $(111)_f$. In fact, Davenport[20] has recently shown that the atomic matching for a lath martensite habit plane very close to $(575)_f$ is much improved by introducing steps with the broad surface $(\bar{1}11)_f \| (0\bar{1}1)_b$ and the step direction parallel to $[\bar{1}01]_f \| [\bar{1}\bar{1}1]_b$ in the habit plane. If that is the case, the Burgers vector lies in the atomic habit plane. From the Burgers vector of the dislocations, $a_f/2\ [0\bar{1}1]$, it follows that the complementary shear plane must be contained in the $[0\bar{1}1]_f$ zone. Since any plane contained in the $[0\bar{1}1]_f$ zone would intersect a step on $(111)_f$ in the direction $[0\bar{1}1]_f$, the dislocations must be in screw orientation on an atomic scale if such a step structure exists. Thus, because a step structure with the broad surface of the steps parallel to $(111)_f \| (011)_b$ is likely to exist, the observed dislocations may be in screw orientation on an atomic scale, although the step structure causes the macroscopic (observed) dislocation line to appear off screw orientation.

It is likely that the observed set of interface dislocations is the only set of misfit dislocations. If there were another set of dislocations having the same line direction as the observed set, but a different Burgers vector, the density of dislocations in a certain interface would vary, depending on the reflection, when imaging is performed by using different reflections. If the density of an actual second set parallel to the observed set were beyond the resolution of the microscope, the contrast of the observed set would also be altered.

The existence of a second set of dislocations having a different line direction, but the same Burgers vector as the observed set is, in principle, possible if the spacing of the dislocations is beyond the resolution of the microscope. However, as it appears difficult to understand how an interface dislocation could glide without being an invariant line, along which martensite and austenite planes meet edge to edge,[10] this possibility appears unlikely since there is only one invariant line.[3,4]

In summary, it is suggested that the observed single set of dislocations is the only set of dislocations, which accommodate the misfit between the martensite and austenite lattices, and accomplish the lattice invariant shear of the phenomenological theories. If so, the conservative movement of the interface requires the dislocations to be in screw orientation on an atomic scale, although a step structure having the broad surface of the steps parallel to $(111)_f$ may make the macroscopic dislocation line appear to be off screw orientation.

In this paper we make no attempt to model the interface on an atomic scale. A detailed description of the interface structure will be given in association with the theoretical approach in a later paper.

V. SUMMARY AND CONCLUSION

The structure of the interface between austenite and lath martensite formed in an Fe-20Ni-5Mn alloy has been investigated. For the first time the misfit dislocation structure comprising a martensitic interface has been observed experimentally, and the conclusions of the investigation can be summarized as follows:

1. The interface contains a single set of parallel dislocations having the Burgers vector $a_b/2\ [1\bar{1}1]_b = a_f/2\ [0\bar{1}1]_f$.
2. The macroscopic (observed) dislocation line direction is close to $[0\bar{5}7]_f$, and the dislocation line deviates by about 10 and 15 deg from the screw orientation in austenite and martensite, respectively. The true spacing of the dislocations may vary between 26 and 63Å.
3. The macroscopic habit plane of the laths, which is close to $(575)_f$, must consist of steps on $(111)_f$ planes on an atomic scale. It then follows that the dislocations must be in screw orientation on an atomic scale, although the step structure makes the macroscopic dislocation line appear to deviate from the screw orientation.
4. The observed interface dislocation array appears to satisfy the requirements for a glissile interface. This suggests that the observed dislocations accommodate the misfit between the martensite and austenite lattices and accomplish the lattice invariant shear of the phenomenological theories.

ACKNOWLEDGMENT

This work was supported by the United States Army Research Office (Durham) under Grant DAAG 29-81-K-0089, and their support is gratefully acknowledged.

REFERENCES

1. J. W. Christian: *The Theory of Transformation in Metals and Alloys—Part I, Equilibrium and General Kinetic Theory*, Pergamon Press, Oxford, 1975, p. 359.
2. G. B. Olson and M. Cohen: *Acta Met.*, 1979, vol. 27, p. 1907.

3. M. S. Wechsler, D. S. Lieberman, and T. A. Read: *Trans. AIME*, 1953, vol. 197, p. 1503.
4. J. S. Bowles and J. K. Mackenzie: *Acta Met.*, 1954, vol. 2, pp. 129, 138, and 224.
5. J. W. Christian and K. M. Knowles: *Proc. Int. Conf. on Solid-Solid Phase Transf.*, Pittsburgh, PA, 1981, H. I. Aaronson, D. E. Laughlin, R. F. Sekerka, and C. M. Wayman, eds., TMS-AIME, Warrendale, PA, in press.
6. S. Mahajan: *Phil. Mag.*, 1972, vol. 26, p. 161.
7. S. Mahajan and G. Y. Chin: *Acta Met.*, 1973, vol. 21, p. 1353.
8. J. A. Venables: *Phil. Mag.*, 1962, vol. 29, p. 1.
9. G. B. Olson: *Acta Met.*, 1981, vol. 29, p. 1.
10. J. W. Christian: *Interfaces—Proc. Int. Conf.*, Melbourne, 1969, R. C. Gifkins, ed., Butterworths, London, 1969, p. 159.
11. G. Baro and H. Gleiter: *Acta Met.*, 1973, vol. 21, p. 1405.
12. M. G. Hall, H. I. Aaronson, and K. R. Kinsman: *Surf. Sci.*,,1972, vol. 31, p. 257.
13. J. W. Matthews: *Surf. Sci.*, 1972, vol. 31, p. 241.
14. M. P. Cassidy, B. C. Muddle, T. E. Scott, C. M. Wayman, and J. S. Bowles: *Acta Met.*, 1977, vol. 25, p. 829.
15. J. M. Rigsbee and H. I. Aaronson: *Acta Met.*, 1979, vol. 27, p. 365.
16. B. P. J. Sandvik and C. M. Wayman: *Metall. Trans. A*, 1983, vol. 14A, p. 809.
17. D. J. H. Cockayne: *J. Microscopy*, 1973, vol. 98, p. 116.
18. P. B. Hirsch, A. Howie, R. B. Nicholson, D. W. Pashley, and M. J. Whelan: *Electron Microscopy of Thin Crystals*, Butterworths, London, 1965, p. 312.
19. P. R. Howell, A. R. Jones, and B. Ralph: *Scripta Met.*, 1976, vol. 10, p. 585.
20. A. T. Davenport: *Proc. Int. Conf. on Solid-Solid Phase Transf.*, Pittsburgh, PA, 1981, H. I. Aaronson, D. E. Laughlin, R. F. Sekerka, and C. M. Wayman, eds., TMS-AIME, Warrendale, PA, in press.